

Layer reconstruction and missing link prediction of multilayer network with *Maximum A Posteriori* estimation

Junyao Kuang* and Caterina Scoglio

Department of Electrical and Computer Engineering,
Kansas State University, Manhattan, KS 66506, USA

(Dated: December 23, 2024)

A multilayer network is composed of multiple layers, where different layers have the same set of vertices but represent different types of interactions. Nevertheless, some layers are interdependent or structurally similar in the multilayer network. In this paper, we present a *maximum a posteriori* estimation based model to reconstruct a specific layer in the multilayer network. The *SimHash* algorithm is used to compute the similarities between various layers. And the layers with similar structures are used to determine the parameters of the conjugate prior. With this model, we can also predict missing links and direct experiments for finding potential links. We test the method through two real multilayer networks, and the results show that the *maximum a posteriori* estimation is promising in reconstructing the layer of interest even with large amount of missing links.

I. INTRODUCTION

Network analysis has been widely used in different areas, such as information diffusion, infectious disease spreading, gene co-expression analysis, and transportation systems. People construct networks to analyze the relations of nodes in the system. Through network analysis, one can improve the robustness of networks or reduce systemic failure rates [1, 2]. For example, epidemiologists can use network analysis to predict the number of people infected by COVID-19 and provide pieces of advice to policymakers at an early stage to curb the spreading of the disease [3]. Also, through network analysis, biologists can detect potential relations between genes within co-expression networks. In gene co-expression networks, it is ubiquitous that multiple layers are constructed through testing various biological activities or functions [4, 5]. However, some edge identification experiments are expensive and time-consuming. Researchers are unable to obtain the entire network with restricted resources in a short period. An alternative way to solve the problem is to reconstruct the layer of interest through the interdependent layers obtained from existing data or simple experiments [8, 12, 13]. After reconstructing the target layer, people can devote restricted resources to the node pairs with high expected number of edges. Various algorithms have been proposed to reconstruct networks and predict missing links [6–11, 14–20], and most of them are based on generative models [21, 22]. In this paper, we will also focus on the generative models.

A stochastic generative model is to model the network structure by fitting the network features to a stochastic block model [8, 14, 15, 23]. To reconstruct the target layer in the multilayer network, we can either use

the target layer solely or take advantage of the structurally similar layers. In [14, 15], the authors presented a degree-correlated stochastic block model to model a single layer network. The authors reconstructed the single layer network by maximizing the likelihood through expectation-maximization algorithm. The method can also help to detect overlapping communities. Paper [8] extended the single layer stochastic block model to multilayer networks and used it to predict missing links and detect overlapping communities. The experiments show that the method is valid when the layers are similar or interdependent. However, when the layers are independent, the authors tried all the layer combinations to find the maximized likelihood. The layers that can improve the maximum likelihood are detected as the interdependent layers. Therefore, when there are numerous layers, it is impossible to try all the layer combinations to find the maximum likelihood. The authors validated the algorithm through two multilayer networks by hiding 20% of links and non-links. In most cases, the number of lost edges is unknown to the people, and the results will be significantly affected by the missing links. The goals of this work are to solve these issues.

To avoid the brute force combination method mentioned above, we will use network comparing methods to detect structurally similar layers or the so-called interdependent layers. We compare the target layer with the other layers when the target layer is partially known to us. The authors [24, 25] compared and discussed the *DeltaCon* method, which compares the similarities of node pairs between two graphs. However, the similarity obtained through this method is highly affected by the number of nodes and links. And there are no universal criteria and threshold to evaluate the similarity between the two networks. Paper [26, 27] compared several network comparing methods. Including vertex/edge overlapping, vertex/edge vector similarity, and signature similarity. Among these comparing methods, the sig-

* Correspondence email address: kuang@ksu.edu

nature similarity is the most promising method. Because people can compare two networks by comparing the network features, such as PageRank [28], eigenvector centrality, betweenness centrality, degree centrality, etc. In this work, we will use the *SimHash* algorithm [26, 27] to compare the layers, which is in the signature similarity family.

In this paper, we present an alternative method for layer reconstruction and missing link prediction. The contributions of this work can be summarized as follows. Inspired by paper [8, 14, 15], we use the *maximum a posteriori* algorithm to reconstruct a target layer in a multilayer network. Similarly, we will use Poisson distribution to derive the posterior probabilities for the layer of interest. And the Gamma distribution is used as the conjugate prior [29]. The adjacency matrices of the interdependent layers are used to determine the parameters of conjugate prior, and the contributions of the layers are weighted by the similarities. In experiments, we show that high similarity layers are critical in improving the robustness of link prediction.

The paper is organized as follows. First, we will derive the *maximum a posteriori* estimation for the layer of interest. Second, we review the *SimHash* algorithm for finding layers with similar features, and we will use the eigenvector centrality for the comparison. Then, we present the method for identifying parameters of conjugate Gamma prior under different circumstances. Finally, we validate the proposed method through two real multilayer networks, and compare the results with the maximum likelihood estimation algorithm.

II. LAYER RECONSTRUCTION IN MULTILAYER NETWORK

A. *Maximum a posteriori* based stochastic block model

In this section, we define the stochastic block model for both directed and undirected multilayer networks. We assume that θ is the parameter set that can reconstruct a layer in the multilayer network. The parameter D is used to denote the adjacency matrix of the target layer. Based on Bayes theorem, we can get the posterior expression for θ as

$$P(\theta | D) = \frac{P(D | \theta)P(\theta)}{P(D)}, \quad (1)$$

where $P(\theta | D)$, $P(D | \theta)$, $P(\theta)$ and $P(D)$ are the posterior probability of the parameter set θ , the likelihood of the network under the parameter set θ , the prior probability of the parameter set θ and the marginal likelihood which contains all the information of the network, respectively. Since $P(D)$ is a constant, so $P(\theta | D)$ is

proportional to the product of $P(D | \theta)$ and $P(\theta)$, and the relation can be derived as

$$P(\theta | D) \propto P(D | \theta)P(\theta). \quad (2)$$

For the nodes in the network, we use E_{ij} to denote the expected number of links (which could be fractional) between node i and node j . So then we have $\theta = \{E_{ij}\}$, for all of the node pairs. We use A_{ij} to denote the adjacency matrix of the target layer. In the undirected and unweighted network, the entries of the adjacency matrix are either 0 or 1.

Before we substitute any parameters into expression (2), we make the following assumptions. The links in the target layer are independent and identically distributed. In other words, the number of edges between node i and node j does not affect the relation between node i and node k . Further, we assume the expected number of links between two nodes is a Poisson distribution. So we can rewrite expression (2) after substituting E_{ij} and A_{ij} as

$$\begin{aligned} P(\{E_{ij}\} | D) &\propto \prod_{i,j} \frac{e^{-E_{ij}} (E_{ij})^{A_{ij}}}{A_{ij}!} P(\{E_{ij}\}) \\ &\propto \prod_{i,j} e^{-E_{ij}} (E_{ij})^{A_{ij}} P(\{E_{ij}\}). \end{aligned} \quad (3)$$

To reconstruct the probabilistic model of the target layer, we need to specify the prior distribution of $P(\{E_{ij}\})$. Since the conjugated distribution for the exponential family is Gamma distribution. i.e.

$$\begin{aligned} P(\{E_{ij}\}) &= \frac{\beta_{ij}^{\alpha_{ij}}}{\Gamma(\alpha_{ij})} E_{ij}^{\alpha_{ij}-1} e^{-\beta_{ij} E_{ij}} \\ &\propto E_{ij}^{\alpha_{ij}-1} e^{-\beta_{ij} E_{ij}}, \end{aligned} \quad (4)$$

where α_{ij} , β_{ij} and $\Gamma(\alpha_{ij})$ are the shape parameter, the scale parameter, and The gamma function of the gamma distribution, respectively. Substituting the above conjugate distribution into expression (3), we obtain

$$P(\{E_{ij}\} | D) \propto \prod_{i,j} e^{-(\beta+1)E_{ij}} (E_{ij})^{A_{ij}+\alpha-1}. \quad (5)$$

So the problem now has been simplified to the *maximum a posteriori* estimation problem, i.e., Finding the parameters E_{ij} that maximize the posterior. However, we still need to specify the expression for E_{ij} . We follow [8] and use the tensors to factorize E_{ij} .

In the multilayer network, we assume there are N vertices. And the target layer has K communities. A membership vector s_{iz} , which represents the outgoing degree of node i within community z , is assigned to each node. Similarly, a membership vector t_{jz} is used to denote the incoming degree of node j within community

z . Moreover, a control vector w_z is used to control the density of links within the community z . Based on the above assumptions, the expected number of edges between node i and j will be the summation of expected links across all the K communities. Which is

$$E_{ij} = \sum_z^K s_{iz} t_{jz} w_z. \quad (6)$$

However, equation (5) is still intractable after we substitute equation (6) into it. After taking the log likelihood of equation (5), we have

$$\begin{aligned} L(\theta | D) &= \sum_{i,j} [(A_{ij} + \alpha_{ij} - 1) \log E_{ij} - (\beta_{ij} + 1) E_{ij}] \\ &= \sum_{i,j} [(A_{ij} + \alpha_{ij} - 1) \log \sum_z^K s_{iz} t_{jz} w_z \\ &\quad - (\beta_{ij} + 1) \sum_z^K s_{iz} t_{jz} w_z], \end{aligned} \quad (7)$$

where $L(\theta | D)$ is the log posterior.

To find the maximized posterior for the expression (7), we apply the Jensen's inequality $\log \bar{x} \geq \log x$ and we can get

$$\begin{aligned} \log \sum_z^K s_{iz} t_{jz} w_z &= \log \sum_z^K q_{ijz} \frac{s_{iz} t_{jz} w_z}{q_{ijz}} \\ &\geq \sum_z^K q_{ijz} \log \frac{s_{iz} t_{jz} w_z}{q_{ijz}} \\ &= \sum_z^K q_{ijz} (\log s_{iz} t_{jz} w_z - \log q_{ijz}). \end{aligned} \quad (8)$$

The equality is satisfied when

$$q_{ijz} = \frac{s_{iz} t_{jz} w_z}{\sum_z s_{iz} t_{jz} w_z}. \quad (9)$$

After leaving out constant terms, equation (7) can be simplified to

$$\begin{aligned} L(\theta | D) &\geq \sum_{i,j,k} [(A_{ij} + \alpha_{ij} - 1) q_{ijz} \log s_{iz} t_{jz} w_z \\ &\quad - (\beta_{ij} + 1) s_{iz} t_{jz} w_z]. \end{aligned} \quad (10)$$

Then if we take the derivation of equation (10), we can get the expressions for s_{iz} , t_{jz} and w_z as

$$s_{iz} = \frac{\sum_j (A_{ij} + \alpha_{ij} - 1) q_{ijz}}{\sum_j (\beta_{ij} + 1) t_{jz} w_z}, \quad (11)$$

$$t_{jz} = \frac{\sum_i (A_{ij} + \alpha_{ij} - 1) q_{ijz}}{\sum_i (\beta_{ij} + 1) s_{iz} w_z}, \quad (12)$$

$$w_z = \frac{\sum_{i,j} (A_{ij} + \alpha_{ij} - 1) q_{ijz}}{\sum_{i,j} (\beta_{ij} + 1) s_{iz} t_{jz}}. \quad (13)$$

Assigning random initial values for s_{iz} , t_{jz} and w_z , then update equation (9), (11), (12) and (13) alternatively. The optimized values for s_{iz} , t_{jz} and w_z can be found until the expressions converged. The maximum posterior is also achieved, when the algorithm converges.

B. Similarity and layer comparison

If the target layer is unknown to the people, this step will be skipped. And we will use the layers that are believed interdependent or similar to determine the parameters of conjugate prior. However, if the adjacency matrix is partially known, the similarity and layer comparison is recommended.

To compare the layers in the multilayer network, the first thing we need to do is extracting the features of the layers [26, 27]. In our experiments, we will use the eigenvector centrality as the feature to compare the layers in the multilayer network. Because the eigenvector centralities measure the influences of nodes on a layer. A node has high eigenvector centrality if the node is connected by plenty of nodes with high eigenvector centrality. Other types of centrality measures such as degree centrality, edge betweenness centrality, or their combinations can also be used according to the purposes of the experiments or types of multilayer networks.

We extract the eigenvector centrality for the nodes within layer r and denote it by an $N \times 1$ vector C_r . The N entries of the vector are the eigenvector centrality values of all the nodes. Then we apply the *SimHash* algorithm to map the feature (eigenvector centrality in our experiments) of the network into binary bits. The procedure for implementing the *SimHash* algorithm is as follows:

1. Generate N different binary numbers with ϕ bits, and store the N binary numbers to a matrix. So we can get an $N \times \phi$ matrix H , where the entries in the matrix are either 0 or 1. Each row of matrix H corresponds to an entry in vector C_r . Accordingly, the eigenvector centralities of the nodes are projected to a ϕ -dimensional space;

2. Obtaining the weighted feature matrix H_r of layer r . We then set all the zeros of H to -1, and multiply each row of matrix H by its corresponding entry in vector C_r . i.e.

$$H_r(i, j) = C_r(i) H(i, j). \quad (14)$$

Each row of matrix H_r represents the weighted digest of a node in layer r . The digest H_r^d for the entire layer r can be obtained through summing up the entries of

H_r across the columns. i.e. $H_r^d(j) = \sum_i^N H_r(i, j)$. The entries of H_r^d are affected by the eigenvector centralities in vector C_r . Finally, we set $H_r^d(j)$ to 1 if $H_r^d(j)$ greater or equal to 0, otherwise set $H_r^d(j)$ to 0;

3. The similarity between layer m and m' is measured by

$$\mu_{m,m'} = 1 - \frac{\text{Hamming}(H_m^d, H_{m'}^d)}{\phi} \quad (15)$$

, where $\text{Hamming}(H_m^d, H_{m'}^d)$ is the Hamming distance.

C. Identify the parameters of the Gamma distribution prior

In the above analysis, we derived the expressions for reconstructing a target layer of a multilayer network. However, the parameters α_{ij} and β_{ij} are yet to be determined. In an L layers multilayer network, different layers have the same set of vertices, but we will only use the layers with similar structures and features. To reconstruct the layer of interest, we consider the problem in two scenarios.

In the first scenario, we assume we have no information about the target layer, i.e., The entries of the adjacency matrix are all zeros. The similarity between the target layer and the rest layers cannot be determined. We will assume the similarities are all one. And calculate the parameters of the Gamma distribution prior as

$$\begin{cases} \alpha_{ij} = \sum_r^{L'} A_{ij}^r \\ \beta_{ij} = L', \end{cases} \quad (16)$$

where r , L' and A_{ij}^r are the r th layer, the layers that we believe similar to the target layer and the adjacency matrix of layer r , respectively. If $\sum_{r \neq m}^L A_{ij}^r$ less than 1, we will set α_{ij} to 1, and set β_{ij} to 100 to make equation (11), (12) and (13) converge.

In this scenario, we do not have any information regarding the layer of interest. i.e. $A_{ij} = 0$. If we take the zeros into the calculation, this equals that we assume zero presences of all the edges in the target layer. To avoid this issue, we take the entries of A_{ij} as the ratio of α_{ij} and β_{ij} , i.e., $A_{ij} = \alpha_{ij}/\beta_{ij}$. The entries are assigned as the average presences of the layer, which we believe similar to the target layer. People can apply this condition to identify the probabilities of links before doing expensive and time-consuming experiments [12, 13]. And researchers can prioritize their experiments according to the link posterior probabilities.

In the second scenario, we assume the entries of A_{ij} are partially known, and there are missing links in the target layer. In this case, we consider using the layers with high similarities to reconstruct the target layer and

predict missing links. More specifically, we use the similarity method introduced above to compare the layers and find the interdependent layers. Then we use the similarities to help us identify the parameters of the Gamma distribution prior.

The parameters of the Gamma distribution prior are obtained through the weighted similarities and expressed as

$$\begin{cases} \alpha_{ij} = \max(\sum_{r \neq m}^{L'} \mu_{m,r} A_{ij}^r, 1) \\ \beta_{ij} = \max(\sum_{r \neq m}^{L'} \mu_{m,r}, \frac{\sum_{r \neq m}^{L'} \mu_{m,r}}{\alpha_{ij}}), \end{cases} \quad (17)$$

where m , L' and $\mu_{m,r}$ are the target layer, the layers that have high similarities with the target layer and the similarity between the layer m and r , respectively. Similarly, if $\sum_{r \neq m}^{L'} \mu_{m,r} A_{ij}^r$ greater than 0 but less than 1, we will set α_{ij} to 1, and set β_{ij} to $\frac{\sum_{r \neq m}^{L'} \mu_{m,r}}{\alpha_{ij}}$ to keep the mean of Gamma distribution unchanged. If α_{ij} equals to 0, we will set α_{ij} to 1, and set β_{ij} to 100 to make the iterations converge.

In this scenario, the layers' contributions are weighted by the similarities. The layers with high similarities are more likely to affect the reconstruction.

III. EXPERIMENTAL VALIDATION

In this section, we validate the method introduced in Part.2. First, the testing layer and the remaining layers are compared through the eigenvector centrality based signature similarity. Second, the effectiveness of the reconstruction process is validated on two real multilayer networks.

the first multilayer network we use to demonstrate our method has nine layers [30]. Each layer represents a highly variable region (HVR). Each node is a malaria parasite gene, and a link is detected if two nodes share an exact match of significant length. The multilayer network has 307 nodes with heterogeneous degree distributions and structures across the nine layers, and the nine layers have a different number of communities in terms of Louvain algorithm[32]. We show the first three layers in Fig. 1(a) through the KiNG software [31].

The FAO (Food and Agriculture Organization) trade network [33] is used to validate the similarity comparison and network reconstruction. The FAO multilayer network is composed of 364 layers, and each layer represents a product. A link is detected if there are tradings of the product between the two countries. We show the first three layers of the FAO network as in Fig. 1(b).

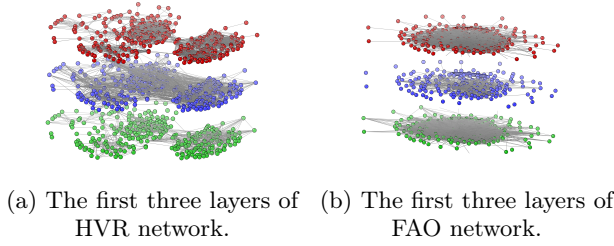


Figure 1: Layer 1, 2, and 3 of the HVR and FAO multilayer network. Same nodes share the same plane coordinates.

A. Validation of the eigenvector centrality based layer comparison

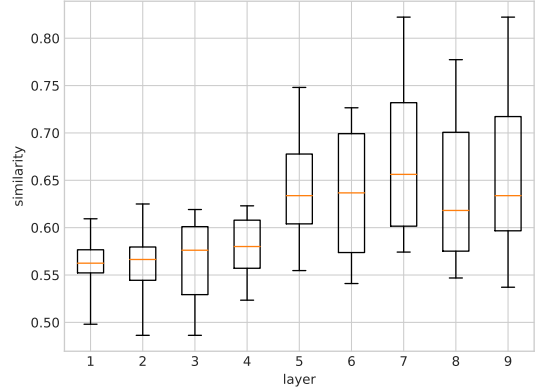
We performed the *SimHash* Algorithm to both the HVR and FAO multilayer networks. The similarities are shown in Fig. 2. Each layer is alternatively set as the target layer, and we compare the target layer with the remaining layers. Therefore, we can get $L - 1$ similarity values for each layer.

The similarity values for each target layer are shown in the interquartile ranges. In figure 2(a), we can see that almost all of the nine layers of the HVR network have similarities less than 0.8, although layer 5, 6, 7, 8, and 9 are closer than layer 1, 2, 3, and 4. Fig. 2(b) shows the similarities of the FAO network. To make it clear, we only showed the results of the first 20 layers. It can be seen that the interquartile ranges of the FAO network are wider since there are more layers. Also, we can observe that the FAO network has more similar layers than the HVR network.

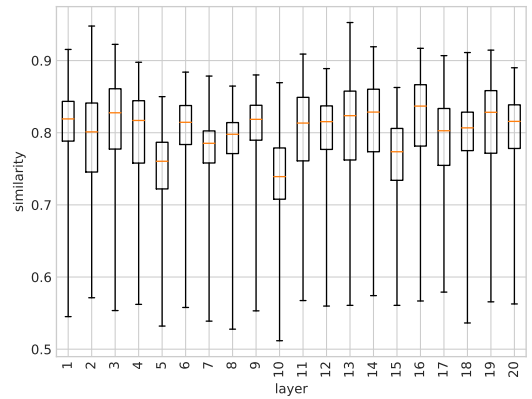
Given a target layer with missing links, people do not know how many links are lost. When we utilize the rest layers to reconstruct the layer of interest, we hope that the similarities vary insignificantly with respect to the missing links. Fig. 3 shows the similarities when the various percent of links removed. We randomly choose three layers to show the results. In the figure, we can see that the similarities do not change much even after we remove 60% and 80% links. This is because the structures of the layers are maintained, and the relative values of the eigenvector centralities do not change significantly. Therefore, the digests of the layers do not change much since they are binary bits determined by the eigenvector centralities.

B. Validation of layer reconstruction and link prediction

The method we presented in this work is mainly for layer reconstruction and missing link estimation. We as-



(a) similarities of the HVR network.

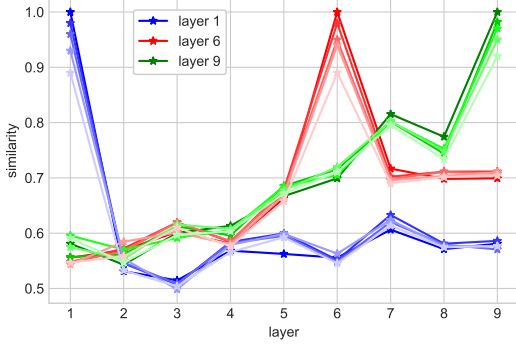


(b) similarities of the FAO network.

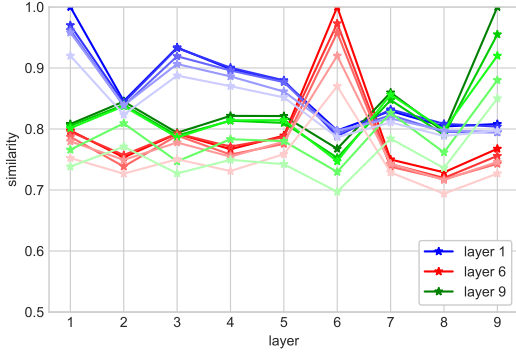
Figure 2: The layer comparison of the HVR and FAO networks. Results are averaged over 10 Monte Carlo cross-validations. Panel a) shows the similarities between each target layer and the remaining layers in the HVR network. Panel b) shows the similarities between the first 20 layers and all the rest layers in the FAO networks.

sume that the relation between the target layer and the rest layers can be pre-assigned or determined through the structural comparison as we introduced above.

Besides, the number of communities K also needs to be specified. The community is not similar to the intuitive communities as detected through traditional methods [34, 35] like the Louvain algorithm [32] or Girvan-Newman algorithm [36]. Since the nodes can belong to multiple communities, and the nodes in these communities have various expected degrees. The parameter w_k is used to control the density of links within different communities. Moreover, there are no sound ways to detect such communities. In this method, we evaluate the



(a) Similarity comparison with edges removed of HVR network.



(b) Similarity comparison with edges removed of FAO network.

Figure 3: Similarity comparison with edges removed. The blue, red, and green represent layers 1, 6, and 9.

The three layers are removed with 20%, 40%, 60%, and 80% links, and then are compared with the layers in the original network. The horizontal axis is the layers in the original network. Lighter color with more links removed. We average the results over 10 Monte Carlo cross-validations.

number of communities by balancing the optimized posterior and computational complexity. Since the vector s_{ik} and t_{jk} are of dimension K , so there are $K + 2NK$ parameters. In each iteration, the computational complexity is $O(N^2K)$. So the time consumed in each iteration is proportional to the number of communities. In the experiments, we input the initial number of communities determined by the Louvain algorithm and find the optimal K by varying the number until the posterior does not improve significantly. Also, we limit the number of communities to less than 20 in considering running time. In practice, we find that the optimized K locates in a wide range, from 10 to 15, the posteriors

are quite close. The results shown in our experiments are all based on ten communities.

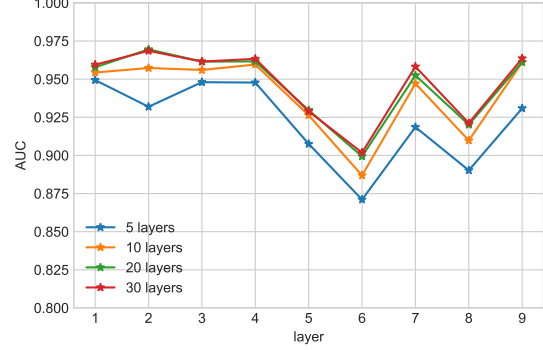


Figure 4: AUCs obtained with different number of similar layers. Results are averaged over 10 Monte Carlo cross-validations.

To evaluate the results, we follow [8, 9, 37] and use the receiver-operator curve (ROC) and the area under the curve (AUC) to validate the effectiveness of our method. The AUC in this method works as follows. Take a value from the set $\{E_{ij}, i < j\}$ as the threshold and we denote it as E_{thres} , we can get the True Positive Rate by comparing the percent of true links with E_{ij} greater than threshold E_{thres} . Similarly, we can discover the False Positive Rate by comparing the percent of non-links with E_{ij} greater than E_{thres} . Repeat the process for all of the values in the set $\{E_{ij}, i < j\}$, and plot the TPR versus FPR. The area under the curve is the AUC. The model is perfect when the AUC approaching 1, and 0.5 means the model is similar to a fair coin tossing.

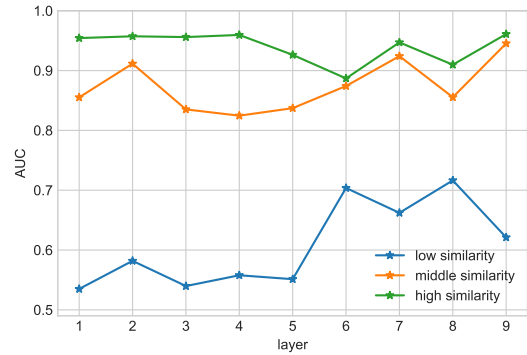
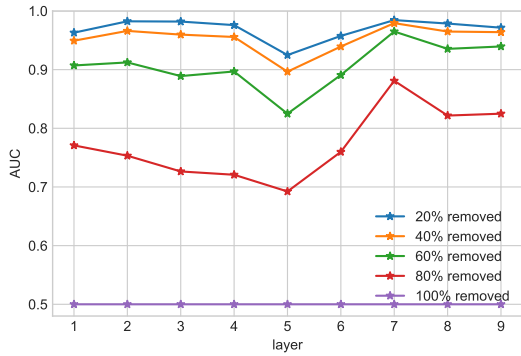


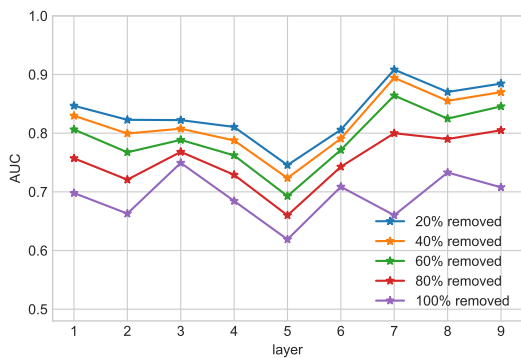
Figure 5: The AUCs were obtained from different similarity ranges. Results are averaged over 10 Monte Carlo cross-validations.

When there are more similar layers, we can get more accurate results. Namely, we can still obtain quite close

results for E_{ij} in the target layer when there are many similar layers, even if we have no data of the target layer. In this experiment, we choose the first nine layers of the FAO network to show the results as there is the same number of layers in the HVR network. And the similarity ranges in the FAO multilayer network are wider. In Fig. 2(b), we know that the similarities between the first nine layers and the rest layers of the FAO network range from 0.5 to 1. To compare how the number of layers affects the results, we choose 5, 10, 20, and 30 layers with highest similarities, respectively. And assume we have no information for the layers of interest as in the first scenario of Part.2(c). The AUCs of the nine layers are shown in Fig. 4. The augmentation of numbers of similar layers enhances the AUCs, but the improvements attenuated as the number of layers is greater than 10. So in the undirected network, ten high similarity layers are enough to help to reconstruct the layer.



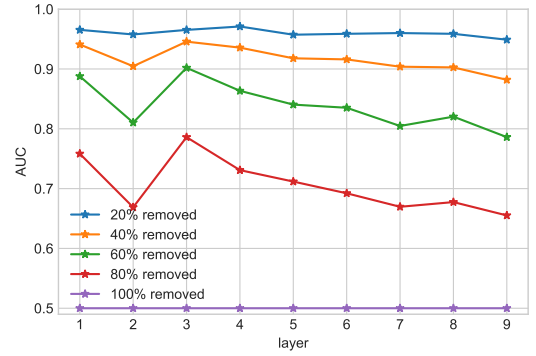
(a) The MLE based AUCs of HVR network.



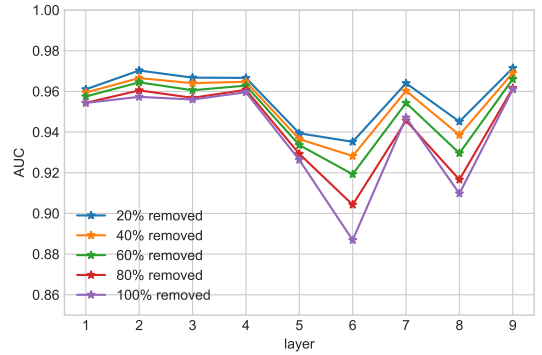
(b) The MAP based AUCs of HVR network.

Figure 6: Comparison of the MLE and MAP methods for the HVR network. Results are averaged over 10 Monte Carlo cross-validations.

Then, we will show that the layers with high similar-



(a) The MLE based AUCs of FAO network.



(b) The MAP based AUCs of FAO network.

Figure 7: Comparison of the MLE and MAP methods for the FAO network, where the 10 layers with highest similarities are used. Results are averaged over 10 Monte Carlo cross-validations.

ities can provide more accurate results. In this experiment, for each target layer, we choose ten layers with highest similarities (greater than 0.8), 10 layers with similarities range from 0.7 to 0.8, and 10 layers with similarities range from 0.6 to 0.7, respectively. Similarly, we use these layers to reconstruct the target layers and show the results in figure 5. The ten layers with high similarities return the best performance. Similarities in the range of 0.7 to 0.8 provide fair good results. In contrast, the ten layers with similarities range from 0.6 to 0.7 produce the worst results. In constructing a target layer in a multilayer network, it is recommended to use the layers with similarities greater than 0.7.

In Fig. 6 and 7, we compared the results obtained through Maximum Likelihood Estimation (MLE) and the *maximum a posteriori* (MAP) estimation. For the layer of interest, we remove 20%, 40%, 60%, 80%, and 100% of links, respectively. We compare the removed network with other layers to obtain the similarities. By

applying the MLE and MAP method, we can obtain the E_{ij} for all the node pairs in the target layer. We then compare the E_{ij} with the original network, which we used as the ground truth. We apply the second scenario as introduced in part two (c) to the 20%, 40%, 60%, and 80% links removed conditions. And apply the first scenario to the 100% links removed condition.

In the HVR network, most of the similarities are less than 0.8, which means the layers are more heterogeneous than the layers in the FAO network. In both Fig. 6(a) and 7(a), the AUCs obtained through the MLE varying with respect to the percent of links removed. In contrast, the ranges of the AUCs obtained through the MAP method are narrower. Especially when the layers are more similar as in Fig. 7(b).

IV. CONCLUSION

To model the layer of interest, we take advantage of the high similarities layers. First, we derived the *maximum a posteriori* estimation for the target layer reconstruction, and used the Gamma distribution as the conjugate prior. Second, we introduced the similarity and layer comparison process. Then, we separated the problem into two scenarios. In the first scenario, if the target layer is unknown to us, we use the layers that are believed to have high similarities. In the second scenario, if the target layer is partially known, we can use the comparing method to find similar layers. The similar layers are then used to determine the parameters of the conjugate prior.

However, there are still some drawbacks to the method we presented. It is required that layers used to find the prior must be similar to the layer of interest. The similarities need to be pre-determined or detected through feature comparisons. Besides, the number of communities needs to be specified. Although various methods have been proposed to detect communities for nodes [32, 34–36]. To our knowledge, there are no sound and reliable ways to obtain multiple communities. In this method, we tested multiple numbers for K , and find the optimal K by balancing the convergence time and maximum posterior. Further, we did not quantify how the number of similar layers combining the target layer affects the posterior. We leave these questions for future works.

The method we proposed shows promising results when we can identify the similarities between the target layer and the supporting layers. The results are less likely affected by the percent of missing links, which is generally unknown to the researchers. On the contrary, the results obtained through the MLE method are significantly affected by the percent of missing links. We believe that the results obtained through our MAP method can help researchers prioritize their experiments, especially when there is no information about the layer of interest.

ACKNOWLEDGEMENTS

This work was supported by the National Institutes of Health under Grant No. 1R01AI140760-01A1.

-
- [1] Q. Yang, D. Gruenbacher, J. L. Heier Stamm, G. L. Brase, S. A. DeLoach, D. E. Amrine, and C. Scoglio, *Physica A* 526, 120856 (2019).
 - [2] Q. Yang, D. Gruenbacher, J. L. Heier Stamm, G. L. Brase, S. A. DeLoach, D. E. Amrine, and C. Scoglio, *PLoS ONE* 15, e0240819 (2020).
 - [3] D. M. Gysi, Í. D. Valle, M. Zitnik, A. Ameli, X. Gan, O. Varol, H. Sanchez, R. M. Baron, D. Ghiassian, J. Loscalzo et al., arXiv:2004.07229.
 - [4] S. Boccaletti, G. Bianconi, R. Criado, C. del Genio, J. Gómez-Gardeñes, and M. Romance, *Phys Rep.* 544, 1 (2014).
 - [5] M. Kivela, A. Arenas, M. Barthelemy, J. P. Gleeson, Y. Moreno, and M. A. Porter, *J Complex Networks*. 2, 203 (2014)
 - [6] R. Guimerà and M. Sales-Pardo, *Proc. Natl. Acad. Sci. U.S.A.* 106, 22073 (2009).
 - [7] S. Boccaletti, G. Bianconi, R. Criado, C. del Genio, J. Gomez-Gardenes, M. Romance, I. Sendina-Nadal, Z. Wang, and M. Zanin, *Phys. Rep.* 544, 1 (2014).
 - [8] C. De Bacco, E. A. Power, D. B. Larremore, and C. Moore, *Phys. Rev. E* 95, 042317 (2017).
 - [9] B. Alfredo, I. Alessandro, and M. A. Paola, *J. R. Soc. Interface* 16, 20180844 (2019).
 - [10] X. Han, Z. Shen, W. X. Wang, and Z. Di, *Phys. Rev. Lett.* 114, 028701 (2015).
 - [11] B. Prasse and P. Van Mieghem, arXiv:1807.08630
 - [12] S. van Dam, U. Vosa, A. van der Graaf, L. Franke, and J. P. de Magalhaes, *Briefings in bioinformatics*, 19, 575 (2018).
 - [13] F. Liesecke, J. O. De Craene, S. Besseau, V. Courdavault, M. Clastre, V. Vergès, N. Papon, N. Giglioli-Guivarc’h, G. Glévarec, O. Pichon et al., *Sci rep.* 9, 14431 (2019)
 - [14] B. Karrer and M. E. Newman, *Phys. Rev. E* 83, 016107 (2011)
 - [15] B. Ball, B. Karrer, and M. E. Newman, *Phys. Rev. E* 84, 036103 (2011)
 - [16] M. E. Newman, *Nature Phys.* 14, 6 (2018).
 - [17] T. P. Peixoto, *Phys. Rev. Lett.* 123, 128301 (2019).
 - [18] T. P. Peixoto, *Phys. Rev. X* 8, 041011 (2018).

- [19] M. E. Newman and E. A. Leicht, Proc. Natl. Acad. Sci. USA 104, 9564 (2007).
- [20] M. E. Newman, Phys. Rev. E 98, 062321 (2018).
- [21] P. Van Mieghem and Q. Liu, Phys. Rev. E 100, 022317 (2019).
- [22] T. P. Peixoto, arXiv:1705.10225.
- [23] T. P. Peixoto, Phys. Rev. E 97, 012306 (2018).
- [24] D. Koutra, N. Shah, J. T. Vogelstein, B. Gallagher, and C. Faloutsos, ACM Trans. Knowl. Discov. Data 10, 28 (2016).
- [25] M. Tantardini, F. Ieva, L. Tajoli, and C. Piccardi, Sci Rep 9, 17557 (2019).
- [26] P. Papadimitriou, A. Dasdan, and H. Garcia-Molina, J. Internet Serv. Appl. 1, 1 (2010).
- [27] M. Charikar, In *Proceedings of the thirty-fourth annual ACM symposium on Theory of computing.* (ACM, New York, 2002), pp:380–388.
- [28] L. Page, S. Brin, R. Motwani, and T. Winograd, Stanford InfoLab. (1999)
- [29] M. C. K. Wu, F. Deniz, R. J. Prenger, and J. L. Gallant, arXiv:1811.01043
- [30] D. B. Larremore, A. Clauset, and C. O. Buckee, PLoS Comput Biol. 9, e1003268 (2013).
- [31] V. B. Chen, I. W. Davis, and D. C. Richardson, Protein Sci. 18, 2403 (2009).
- [32] V. D. Blondel, J. L. Guillaume, R. Lambiotte, and E. Lefebvre, J. Stat. Mech. P10008 (2008).
- [33] M. De Domenico, V. Nicosia, A. Arenas, and V. Latora, Nature comms. 6, 6864 (2015).
- [34] S. Fortunato and D. Hric, Phys. Rep. 659, 1 (2016).
- [35] M. E. J. Newman, Phys. Rev. E 74, 036104 (2006).
- [36] M. Girvan and M. E. Newman, Proc. Natl. Acad. Sci. USA 99, 7821 (2002).
- [37] A. Clauset, C. Moore, and M. E. Newman, Nature 453, 98 (2008)